Heliyon 11 (2025) e42500

Contents lists available at ScienceDirect

Heliyon

journal homepage: www.cell.com/heliyon

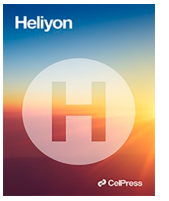

Research article

CO_2 monitoring in non-invasive ventilation (NIV) helmets: A bench study assessment of sensor integration

Camilla Gironi [a], Ramin Amiri [b], Marco Giacinti Baschetti [b], Cristiana Boi [b,c], Laura Cercenelli [a,*], Barbara Bortolani [a], Emanuela Marcelli [c,d]

[a] Laboratory of Bioengineering – eDIMES Lab, Department of Medical and Surgical Sciences (DIMEC), University of Bologna, Bologna, Italy
[b] Department of Civil, Chemical, Environmental, and Materials Engineering (DICAM), University of Bologna, Bologna, Italy
[c] Health Sciences and Technologies – Interdepartmental Center for Industrial Research (CIRI-SDV), University of Bologna, Bologna, Italy
[d] IRCCS Azienda Ospedaliero-Universitaria di Bologna, Bologna, Italy

ARTICLE INFO

Keywords:
Helmet
Noninvasive ventilation
NIV
Acute respiratory failure
Carbon dioxide rebreathing
CO_2 sensor

ABSTRACT

Noninvasive ventilation (NIV) is a well-established technique for managing acute respiratory failure in various clinical settings. However, safety concerns in clinical NIV applications emerge due to the absence of robust monitoring and alarm systems, potentially leading to issues such as CO_2 rebreathing during flow-block events. This work aims to enhance the safety and monitoring of NIV systems by studying the integration of two types of carbon dioxide (CO_2) sensors within NIV helmets. The investigation encompasses two main analyses. The first analysis explores the impact of varying the fresh inlet gas flow rate on local CO_2 concentrations within the helmet. The second analysis investigates the response of CO_2 sensors during simulated flow-block events, a critical safety concern in NIV therapy. In both analyses the effect of the sensor positioning is also investigated. Results demonstrate that higher fresh gas flow rates enhance CO_2 washout within the helmet, highlighting the importance of optimizing gas flow rates to mitigate CO_2 rebreathing. The positioning of CO_2 sensors within the helmet was also found to significantly influence measurements by affecting signal stability and response to flow-block events. Overall, this study demonstrated the potential of integrating CO_2 sensors within NIV helmets to enhance patient safety and treatment effectiveness. The knowledge gained from this study can be used to guide the design and optimization of NIV systems.

1. Introduction

Noninvasive ventilation (NIV) is widely used to support ventilation and oxygenation in patients with respiratory failure. This technique delivers positive pressure to the patient through interfaces like facemasks or helmets, without the need for invasive endotracheal intubation. In recent years, NIV has become a common approach for efficiently and non-invasively treating patients with hypercapnic and hypoxemic acute respiratory failure (ARF) [1]. In addition, NIV is also used to prevent complications like ventilator-associated pneumonia from invasive ventilation and is beneficial in the perioperative setting [2,3]. Moreover, NIV is recommended for patients with weakened immunity as a preventive measure post-extubation and has become essential for managing COVID-19 patients needing respiratory support without intubation [4–8].

* Corresponding author.
E-mail address: laura.cercenelli@unibo.it (L. Cercenelli).

https://doi.org/10.1016/j.heliyon.2025.e42500
Received 26 March 2024; Received in revised form 30 January 2025; Accepted 5 February 2025
Available online 5 February 2025
2405-8440/© 2025 The Authors. Published by Elsevier Ltd. This is an open access article under the CC BY license (http://creativecommons.org/licenses/by/4.0/).

Available NIV modes include continuous positive airway pressure (CPAP) and pressure support ventilation (PSV) [9,10]. The former uses continuous positive end-expiratory pressure (PEEP) to increase functional residual capacity and open flooded alveoli, but does not alleviate inspiratory muscle work, leaving tidal ventilation dependent on respiratory muscles [11–13]. In contrast, PSV mode assists spontaneous breathing by delivering a set inspiratory pressure when triggered, cycling to expiration as inspiratory flow decreases, allowing patients to control their breathing rate and duration [14].

Commercially available interfaces can be classified based on their design and the anatomical structures to which they relate. Among these, facemasks are frequently preferred, however, they may be responsible for CO_2 rebreathing, air leaks, and discomfort at higher pressures, and may be intolerable due to issues like facial ulcers or claustrophobia [15,16]. These challenges contribute to NIV failure, which occurs in 8 % of hypercapnic and 50 % of hypoxemic patients [17,18]. Given that patient comfort is the primary determinant of success in NIV treatment [19], it is crucial to select an appropriate interface type tailored to the individual patient's needs to ensure effective treatment outcomes. An alternative is the helmet interface, which features a transparent hood with a soft neck seal, reducing air leaks and improving tolerability by avoiding direct facial contact [5,20]. However, the helmet interface has a larger internal volume than facemasks and creates a semi-enclosed environment, mixing exhaled gas with fresh gas from the inspiratory limb of the circuit [15,21]. This may lead to CO_2 rebreathing, when the patient's exhaled CO_2 does not completely leave the NIV system with each breath. Instead, it mixes with the internal volume of the helmet and is re-inhaled [22]. Therefore, it is essential to ensure proper CO_2 washout when using the helmet. In such an environment, assuming a homogeneous distribution of CO_2, it has been demonstrated that reducing the size of the helmet does not prevent CO_2 rebreathing, suggesting that the amount of CO_2 produced by the patient and the fresh gas flowing through the helmet are the primary factors determining CO_2 rebreathing [23].

The production of CO_2 is crucial for assessing NIV safety and effectiveness, as exhaled CO_2 indicates ventilation and perfusion efficiency [24]. Persistent respiratory issues can raise blood CO_2 and lower exhaled CO_2. Early studies using helmets for respiratory treatment showed that the arterial partial pressure of carbon dioxide ($PaCO_2$) decreased to normal levels within 24 h of CPAP therapy, suggesting improved clinical outcomes due to respiratory muscle unloading and reduced $PaCO_2$ [4,21,25].

Safety concerns arise with NIV helmet systems due to the lack of reliable monitoring and alarms. Disruptions in gas supply or circuit blockages can cause reduced airflow, increased CO_2 rebreathing, and potential asphyxiation [6]. Discontinuing flow in ARF patients can be fatal, so NIV helmets should be used with proper monitoring and supervision. Helmets include features like a large volume, low resistance inlet, and an "anti-suffocation valve" that opens during flow-block events to mitigate risks. However, this valve may not sufficiently limit CO_2 rebreathing in hypercapnic patients, potentially leading to hypercapnic coma [26]. Recent studies estimate tidal volume during CPAP underscoring the importance of monitoring respiratory parameters [27,28]. The integration of different monitoring tools during NIV treatment could significantly enhance patient care. This is particularly relevant for NIV helmets, where monitoring respiratory variables can be challenging and combining multiple monitoring approaches could yield more reliable and comprehensive results.

In this work, we propose embedding small CO_2 sensors inside a commercial NIV helmet for monitoring its functioning. Our first aim is to determine the CO_2 concentration measured at specific locations inside the helmet under different fresh gas flow rate conditions. This analysis is intended to identify the optimal location of the CO_2 sensor for monitoring the helmet functionality at different fresh gas flow rates. Our second aim is to evaluate the local CO_2 concentration increase inside the helmet during a flow-block event occurring when the fresh inlet gas flow rate stops entering the helmet. This analysis aims to determine the capability of each CO_2 sensor to detect an increase in the local CO_2 concentration inside the helmet following the flow-block. This sensorization, coupled with an alarm system, aims to improve early detection of helmet malfunctions and reduce CO_2 rebreathing risks during NIV treatment.

2. Materials and methods

A commercial NIV helmet was considered for bench testing. The chosen system was a StarMed CaStar Up (Intersurgical, Mirandola, Modena, Italy) characterized by an internal volume equal to 16 L and equipped with an anti-suffocation valve and two auxiliary ports positioned on the anterior side of the helmet front wall. For the tests, the inlet port of the helmet was connected to a blower (VT900A Gas Flow Analyzer Tester, Fluke Biomedical, Fluke Corporation, Everett, Washington, United States) enabling a continuous supply of fresh gas to enter the helmet, while an anti-bacterial filter and a PEEP valve were connected to the outlet port of the helmet. A

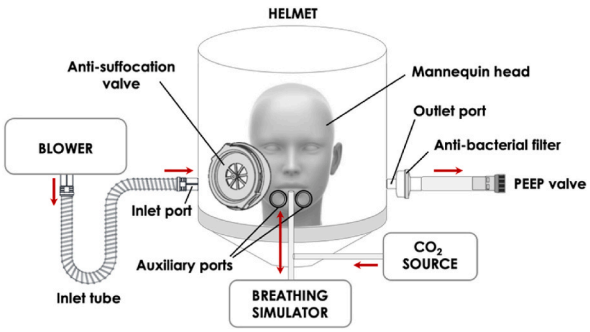

Fig. 1. Experimental setup employed for the bench testing. Red arrows indicate the air flow.

mannequin head was placed inside the helmet to mimic the normal working conditions. The mannequin's mouth was connected to an external breathing simulator (ID AT261, NS Sistemi Integrati, Modena, Italy). The breathing simulator was composed of a closed chamber containing the respiration gas and a piston connected to an external CO_2 gas source. During inspiration the piston moves back thus drawing gas from inside the helmet, while during the exhalation the piston moves forward delivering the gas harvested inside the closed chamber of the breathing simulator to the helmet. The CO_2 source connected to the lung simulator allows the addition of a desired constant amount of CO_2 to the exhaled gas volume entering the helmet during exhalation, according to pre-set derived from the flowmeter within the breathing simulator. A schematic representation of the experimental setup is reported in Fig. 1.

Two distinct Non-Dispersive Infra-Red (NDIR) CO_2 sensors were employed within the study [29]. The first sensor was the SCD30 (Sensirion AG, Switzerland) that is characterized by a cost-effective design and operates at a sampling frequency of one sample every 2 s, with a response time of less than 20 s. Besides, the SprintIR-6s (Gas Sensing Solutions, Cumbernauld, Glasgow, United Kingdom) comes at a comparatively higher cost but offers a significantly higher sampling frequency of 20 samples per second, accompanied by a rapid response time, typically ranging from 3 to 4 s. In view of the varying attributes of these sensors, we chose to employ the SCD30 sensor for monitoring local CO_2 concentrations within the helmet by positioning it on the side wall of the helmet close to the outlet port to intercept the CO_2 emitted by the mannequin's mouth. On the other hand, we dedicated the SprintIR-6s sensor to measure CO_2 concentrations in the region of the helmet closest to the mannequin's mouth, with the aim of evaluating rapid fluctuations in CO_2 levels within the exhaled volume, which are impossible to capture with the SCD30 sensor.

Fig. 2 provides an illustration of the different locations considered for the placement of the CO_2 sensors within the helmet.

Four SCD30 sensors (designated as A, B, C, and D) were positioned on the wall of the helmet near the outlet port as indicated in Fig. 2. The selected areas for positioning of the CO_2 sensors ensure that the sensors do not interfere with the two auxiliary access ports and allow the patient to rest his head on the pillow. An additional SCD30 sensor (labeled as E) was connected to the outlet tube for monitoring the CO_2 concentration in the gas leaving the helmet. According to the manufacturer's guidelines, each SCD30 sensor was lodged inside a customized 3D-printed housing, manufactured using Form 2 printer (Formlabs, Somerville, MA, United States), which was connected to the helmet. The housings were securely connected to the helmet by creating dedicated openings at specific locations facilitating gas exchange between the interior of the housing and the inner space of the helmet. Indeed, this design guaranteed that the gas to be analyzed could pass through the housing containing the CO_2 sensor without the sensor directly interacting with the gas flow inside the helmet. To integrate the SprintIR-6s sensor (designated as F), the left auxiliary port of the helmet was utilized. One of the two connectors of the sensor was linked to the auxiliary port using a small plastic tube, while the other remained open to the external environment. This setup was designed to ensure a unidirectional flow through the sensor, meaning that air would pass from inside the helmet through the sensor and then exit into the external environment. It should be noted that for both sensors an anti-bacterial filter was inserted between the sensor and the internal space of the helmet to mitigate the potential risk of sensor contamination, especially crucial when treating patients with contagious disease. Fig. 3a and Fig. 3b provide visual representations of how SCD30 and SprintIR-6s sensors were connected to the helmet.

Each CO_2 sensor was connected to a PC via Arduino – UNO R3 boards (https://www.arduino.cc) for data acquisition and communication. Moreover, each sensor was properly calibrated before the experimental campaign.

The sensors were employed to monitor the CO_2 concentration inside the helmet under different NIV working conditions. Two investigations were conducted to accomplish this goal. The first analysis (Analysis 1) focused on the effect of varying fresh inlet gas flow rates on the local CO_2 concentration within the helmet. The second analysis (Analysis 2) was designed to examine the response of the CO_2 sensors during a simulated flow-block event, which is a critical safety concern in NIV therapy.

2.1. Analysis 1

The effect of different fresh gas flow rates on the local CO_2 concentration was tested. We increased the fresh inlet gas flow rate of the blower from 50 L/min to 90 L/min in 10 L/min steps. The respiration parameters were maintained constant as follows: respiration rate (RR) of 28 breaths per minute (bpm), inspiratory to expiratory (I:E) ratio of 1:1, and tidal volume of 500 mL. The CO_2 flow rate introduced into the respiration volume was maintained constant at 0.31 L/min. The PEEP valve was manually regulated to ensure an

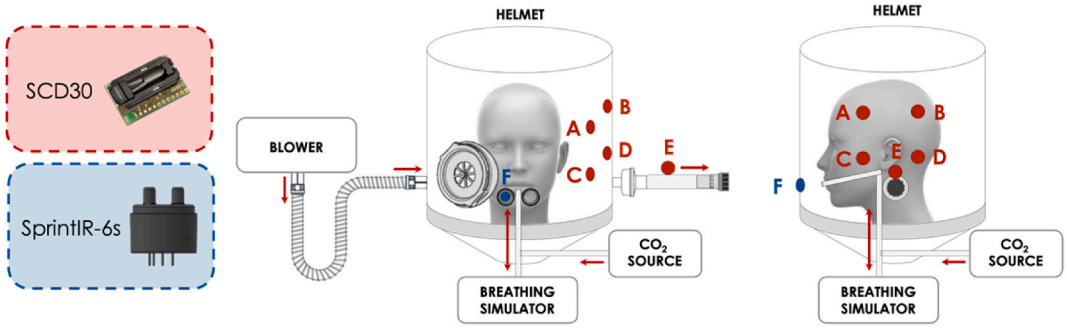

Fig. 2. Frontal view (left) and lateral view (right) depict the positions chosen for CO_2 sensors within the helmet. Red circles (A, B, C, D, E) denote the placement of SCD30 sensors, while blue circles (F) indicate the location of the SprintIR-6s sensor. Red arrows indicate the air flow.

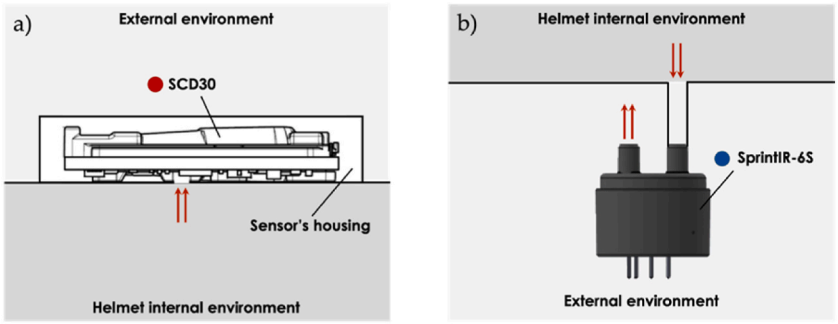

Fig. 3. CO_2 sensors' connections to the helmet for real-time CO_2 monitoring: (a) SCD30 sensor and (b) SprintIR-6s sensor. Red arrows indicate the air flow.

end-expiration pressure of 7.5 cmH_2O.

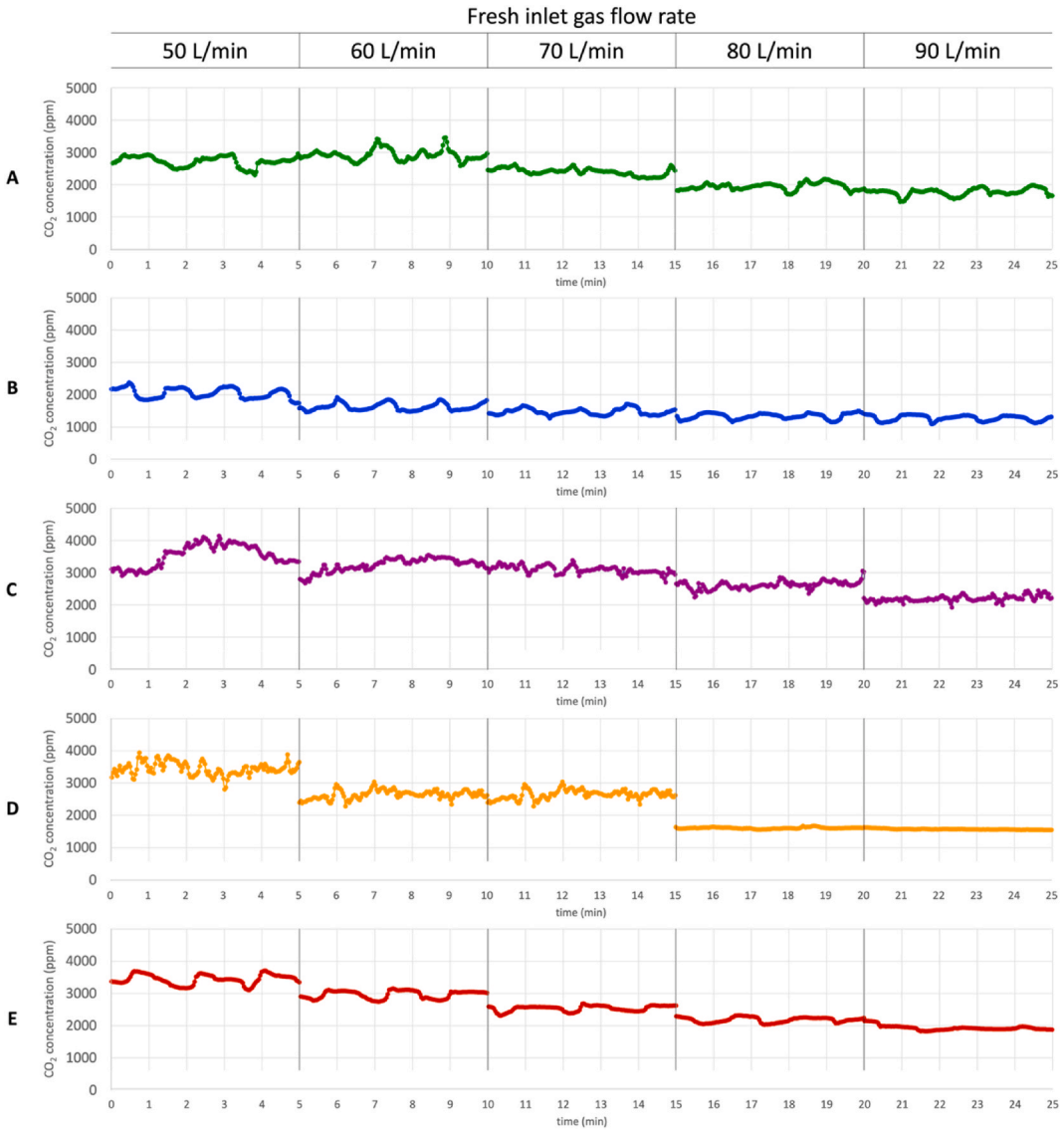

Fig. 4. CO_2 concentration signals acquired with the SCD30 sensors placed in different positions inside the helmet: A (green), B (blue), C (purple), D (orange), and E (red) in response to increasing fresh inlet gas flow rates.

2.2. Analysis 2

The impact of a flow-block event, which occurs when the blower ceases operation while the inlet tube remains connected to the helmet, was assessed. We started with an inlet flow rate of fresh gas equal to 90 L/min and then, once the sensor signal was stable, we dropped it to 0 L/min. The respiration parameters were maintained equal to the ones used in Analysis 1. The local CO_2 concentration inside the helmet was recorded for 5 min after starting the flow-block.

2.3. Statistical analysis

We conducted a statistical analysis using STATA/SE version 18.0 (StataCorp LLC, Texas, United States) to thoroughly examine and evaluate the research findings. The Student's t-test was used for pairwise comparisons between two groups, which provides a robust method for assessing the statistical significance of differences in means between the groups [30]. A p-value of <0.05 was considered statistically significant.

Furthermore, in the context of Analysis 1 data, linear regression analysis was employed to examine the CO_2 concentration mean values across various fresh gas flow rates, and the coefficient of determination (R^2) was subsequently determined to quantify the goodness of fit of the regression model.

3. Results

3.1. Analysis 1

The CO_2 measurements obtained with the SCD30 sensors for different fresh inlet gas flow rates are shown in Fig. 4. Five-minute-long acquisitions are reported for each flow rate value.

Fig. 5 shows, for each SCD30 sensor, the dependency of the mean value and standard deviation of CO_2 concentration on the applied fresh inlet gas flow rate.

The Student's t-test was employed to assess statistical differences in CO_2 concentration measurements obtained at consecutive fresh gas flow rates values. The resulting p-values from this analysis are detailed in Table 1.

The results of the linear regression analysis indicated varying goodness-of-fit, as reflected by the R^2 values: 0.92 for sensors A and B, 0.86 for sensor C, 0.87 for sensor D, and 0.96 for sensor E.

The CO_2 concentration measurements obtained with the SprintIR-6s sensor for different fresh inlet gas flow rates are shown in Fig. 6. Ten-second-long acquisitions are reported for each flow rate value.

The acquired CO_2 concentration signals exhibit distinct oscillations, with peak values observed at the end-exhalation phase and minimum values occurring at the end-inspiration phase.

Fig. 7 reports, for the SprintIR-6s sensor, the dependency of the CO_2 concentration mean values and standard deviations, calculated at both the end-exhalation and end-inspiration phases, on the applied fresh inlet gas flow rate.

The Student's t-test was employed to assess statistical differences in CO_2 concentration measurements obtained at consecutive fresh gas flow rates values. The resulting p-values from this analysis are detailed in Table 2. The results of the linear regression analysis indicated R^2 values of 0.97 for the end-exhalation data and 0.88 for the end-inhalation data.

3.2. Analysis 2

Fig. 8 depicts the local CO_2 concentration acquired with SCD30 sensors A, B, C, D, and E before and after flow-block onset. Five-minute-long acquisitions are reported after the fresh inlet gas flow rate drops to 0 L/min.

For each SCD30 sensor, we assessed the percentage variation of CO_2 concentration ($\Delta CO_2\%$) as the relative difference between the

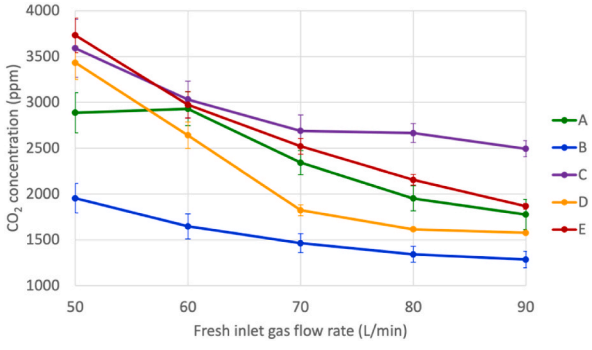

Fig. 5. Effect of increasing fresh inlet gas flow rate on CO_2 concentration measured with SCD30 sensors A (green), B (blue), C (purple), D (orange), and E (red).

Table 1
P-values resulting from Student's t-test analysis for CO_2 concentration measurements acquired with SCD30 sensors A, B, C, D, E.

Fresh inlet gas flow rate (L/min)	A	B	C	D	E
50–60	0.97	0.00	0.00	0.00	0.00
60–70	0.00	0.00	0.00	0.00	0.00
70–80	0.00	0.00	0.00	0.00	0.00
80–90	0.00	0.00	0.00	0.00	0.00

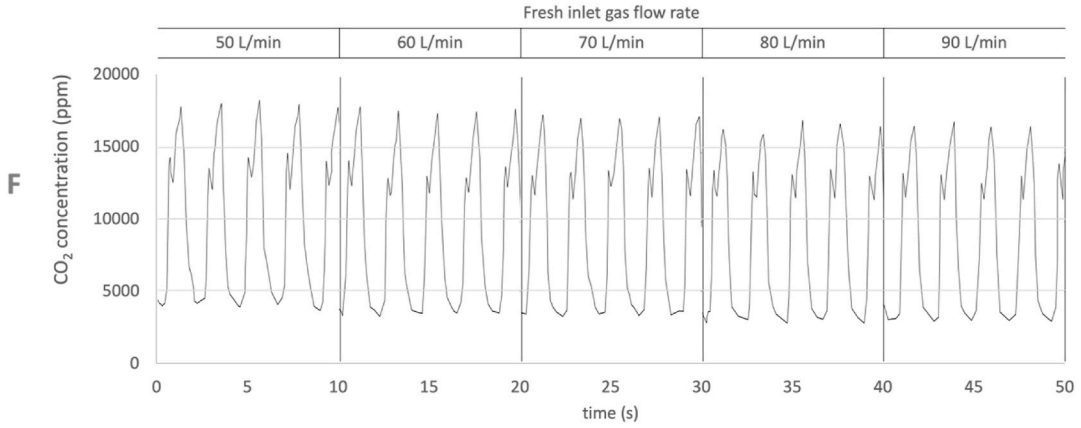

Fig. 6. CO_2 concentration signals measured with the SprintIR-6s sensor for increasing fresh inlet gas flow rates.

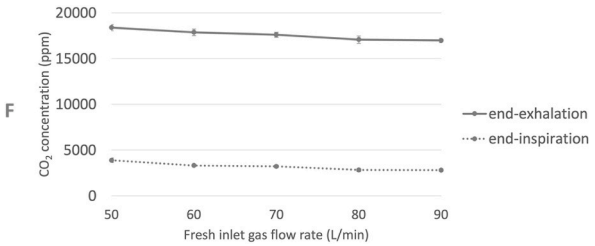

Fig. 7. CO_2 concentration mean values and standard deviations acquired with the SprintIR-6s for increasing fresh inlet gas flow rates. The solid line illustrates the end-exhalation values, while the dotted line represents the end-inspiration ones.

Table 2
P-values resulting from Student's t-test analysis for CO_2 concentration measurements acquired with SprintIR-6s sensor at the end-exhalation (F_{eE}) and end-inspiration (F_{eI}) phases.

Fresh inlet gas flow rate (L/min)	F_{eE}	F_{eI}
50–60	0.00	0.00
60–70	0.03	0.01
70–80	0.00	0.00
80–90	0.27	0.63
Fresh inlet gas flow rate (L/min)	F_{eE}	F_{eI}
50–60	0.00	0.00
60–70	0.03	0.01
70–80	0.00	0.00
80–90	0.27	0.63

CO_2 concentration measured at selected minutes following the initiation of the flow-block (denoted as MX) and the last CO_2 measurement obtained just before the flow-block onset (referred as M0). To enhance robustness, we calculated the mean value of CO_2(M0) based on five samples taken immediately before the onset of the flow block, while for the CO_2(MX) values, we determined the mean value from five samples centered around the selected time. The ΔCO_2% is calculated following Equation (1).

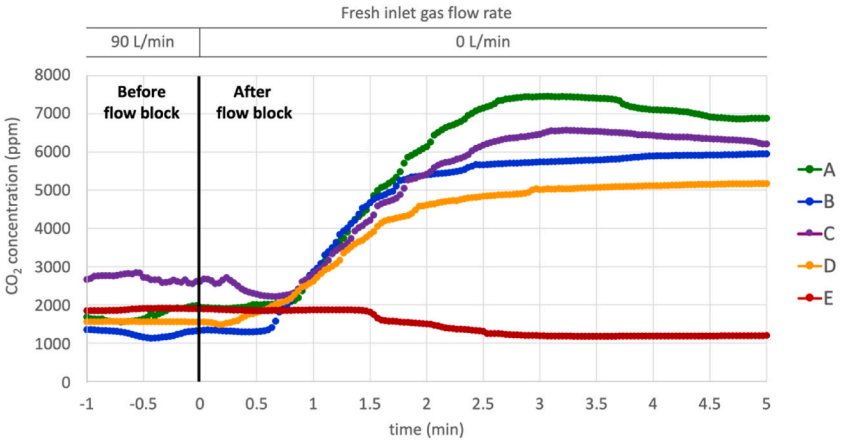

Fig. 8. CO_2 concentration during a flow-block event (black line: flow-block starts) acquired with SCD30 sensors A (green), B (blue), C (purple), D (orange), and E (red).

$$\Delta CO_2\% = \frac{CO_2(MX) - CO_2(M0)}{CO_2(M0)} * 100 \quad (1)$$

Fig. 9 shows, for each SCD30 sensor, the $\Delta CO_2\%$ values calculated at 30-s intervals following the initiation of the flow-block event.

The assessment of statistical differences in CO_2 concentration measurements collected over time was conducted using the Student's t-test, employing a time step of 0.5 min. The resulting p-values are detailed in Fig. 10 represents the CO_2 measurements obtained with the SprintIR-6s sensor immediately before and 5 min after flow-block starts. Ten-second-long acquisitions are reported for each condition.

We adapted the previously established definition of $\Delta CO_2\%$ to accommodate the SprintIR-6s sensor's data. In detail, we defined the average percentage variation of CO_2 concentration ($\overline{\Delta CO_2}\%$) as the percentage variation of the relative difference between the mean CO_2 concentration at 5 min after flow-block onset (M5) and the mean CO_2 concentration before the flow-block starts (M0). Mean CO_2 concentration values are calculated over 12 respiratory cycles at both end-exhalation ($\overline{\Delta CO_{2_{eE}}}\%$) and end-inspiration ($\overline{\Delta CO_{2_{eI}}}\%$) following Equations (2) and (3) respectively.

$$\overline{\Delta CO_{2_{eE}}}\% = \frac{\overline{CO_{2_{eE}}(M5)} - \overline{CO_{2_{eE}}(M0)}}{\overline{CO_{2_{eE}}(M0)}} * 100 \quad (2)$$

$$\overline{\Delta CO_{2_{eI}}}\% = \frac{\overline{CO_{2_{eI}}(M5)} - \overline{CO_{2_{eI}}(M0)}}{\overline{CO_{2_{eI}}(M0)}} * 100 \quad (3)$$

The calculated $\overline{\Delta CO_{2_{eE}}}\%$ and $\overline{\Delta CO_{2_{eI}}}\%$ values are 39 % and 70 % respectively.

P-values obtained from the Student's t-test analysis, comparing CO_2 concentration variations between M0 and M5, indicate

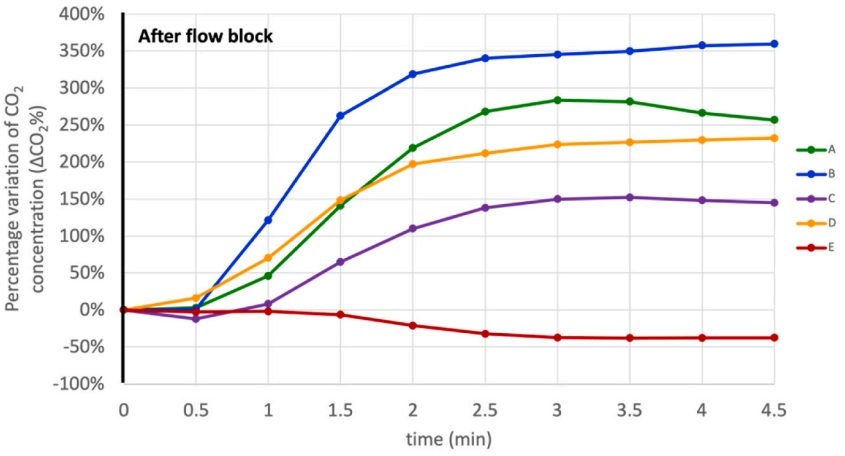

Fig. 9. Percentage variation of CO_2 concentration ($\Delta CO_2\%$) after flow-block measured with SCD30 sensors. The $\Delta CO_2\%$ values are calculated at 30-s intervals following the onset of the flow-block event.

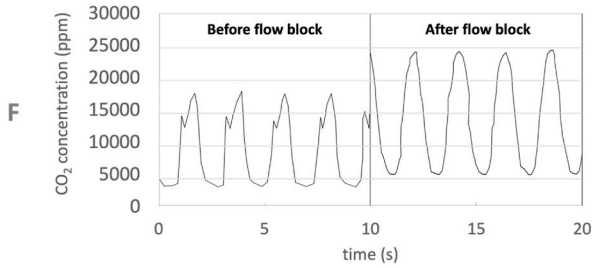

Fig. 10. CO_2 concentration before (left) and after (right) flow-block event acquired with SprintIR-6s sensor (black line: flow-block starts).

statistical significance with a p-value of 0.00 for both end-exhalation and end-inspiration values.

4. Discussion

4.1. Analysis 1

Almost all SCD30 sensors exhibited a statistically significant reduction in local CO_2 concentration with respect to the increasing fresh inlet gas flow rate entering the helmet (Fig. 4), as demonstrated by the Student's t-test analysis results shown in Table 1. The only exception was observed for sensor A when passing from 50 L/min to 60 L/min ($p = 0.97$). This finding aligns with prior research, supporting the notion that higher flow rates passing through the helmet result in more effective washout behavior [4,15,21,22,31]. Furthermore, the acquired CO_2 concentration signals exhibit periodic oscillations, as evidenced in Fig. 4. We hypothesize that these oscillations may arise from several factors: the mismatch between the SCD30 sensor's sampling frequency and respiratory frequency, noise from the breathing simulator's pump system, and fluctuations in local CO_2 concentrations due to turbulent flow inside the helmet. These factors affect both the recorded CO_2 levels and their temporal variations, though a complete understanding of the phenomenon is still lacking.

Fig. 5 reports the relationship between the mean local CO_2 concentration acquired with the SCD30 sensors with respect to their positioning inside the helmet. The results suggest a strong dependence of the measured CO_2 concentration on the position of the sensors. Sensor A shows a non-monotonic decreasing trend since it is characterized by an initial increment in its output response as the flow rate increases from 50 L/min to 60 L/min, succeeded by a subsequent decline as the flow rate further rises to 70 L/min. In contrast, all the other sensors (i.e., sensor B, C, D and E) show a monotonic decreasing trend. The linear regression has revealed, especially for sensor E, an almost linear behavior, given the high values of the coefficient of determination R^2. This suggests the possibility of correlating the CO_2 concentration with the fresh inlet gas flow rate values. Fig. 5 shows that sensors A, B, and E have lower stability, with standard deviations under 200 ppm, while sensors C and D have higher standard deviations, below 400 ppm. This suggests that the upper section of the helmet experiences slower CO_2 concentration variations due to less turbulence, whereas sensor E, located on the outlet tube, faces more turbulent flow, causing abrupt CO_2 concentration fluctuations.

As depicted in Fig. 6, the high sampling rate of the SprintIR-6s sensor allows the real-time monitoring of rapid fluctuations in local CO_2 concentration near the mannequin's mouth during the breathing cycle. The acquired signal reaches its maximum values at the end-exhalation phase since the exhaled gas volume that contains a high CO_2 concentration enters the sensor inlet located near the mannequin's mouth. Conversely, during inspiration, the gas volume passing through the sensor contains a low CO_2 concentration, resulting in a decrease of the acquired signal reaching the minimum values. As the fresh inlet gas flow rate increases, both the maximum and minimum values of the CO_2 concentration signal decrease, as a consequence of the helmet's improved washout capability which efficiently eliminates the accumulated CO_2 within the helmet. The observed trend achieved statistical significance ($p < 0.05$), as determined by the Student's t-test, for fresh inlet gas flow rate transitions from 50 L/min to 60 L/min, from 60 L/min to 70 L/min and from 70 L/min to 80 L/min. However, it was observed a non-significant decrease when passing from 80 L/min to 90 L/min (p-values equal to 0.27 for end-exhalation and 0.63 for end-inspiration values). This implies that, due to the SprintIR-6s sensor proximity to the mannequin's mouth, the washing effects from the incoming flow into the helmet are less pronounced compared to those observed with the SCD30 sensors.

4.2. Analysis 2

The response of the SCD30 sensor to a flow-block event, as illustrated in Fig. 8, is strictly related to the positioning of the sensors inside the helmet. In particular, the sensors placed on the wall of the helmet (i.e., sensors A, B, C, D) exhibit an increase in the CO_2 concentration measurement when the flow-block occurs, indicating CO_2 accumulation inside the helmet. In contrast, the sensor positioned on the outlet tube of the helmet (i.e., sensor E) registers a decrease in the CO_2 concentration measurement after the flow-block initiates. In this scenario, the driving force at the outlet port of the helmet, which is typically represented by the PEEP value maintained during the proper functioning of the NIV system, is lost due to the opening of the anti-suffocation valve, causing a reduction in the internal pressure within the helmet. Consequently, the PEEP valve closes, disrupting the airflow coming from inside the helmet through the outlet tube.

The Student's t-test results, reported in Table 3, revealed a statistically significant increase in local CO_2 concentration within the initial 30 s after a flow block for sensor A and D, while after 1 min this significance is extended also to sensor B and C. This observed trend is then maintained for the rest of the acquisition. Conversely, sensor E exhibits a statistically significant decrease in local CO_2 concentration within 30 s after the initiation of the inlet flow interruption. These findings suggest that all sensors positioned on the helmet front wall (i.e., sensors A, B, C and D) consistently demonstrate a good capability to detect reliable CO_2 variations following a flow-block, with timing suitable for integration into an alarm system.

Considering the percentage variations in CO_2 concentration measurements depicted in Fig. 9, sensor B exhibits the highest sensitivity to the blockage of incoming fresh gas flow rate. Indeed, after 1 min since the flow-block starts, sensor B records an increase in the local CO_2 concentration of 121%, which becomes higher than 300% from the second minute onwards. Sensor A also shows a high percentage variation in CO_2 concentration after the flow-block, reaching 284% in the first 3 min. Instead, sensors C and D detect a more gradual rise in CO_2 concentration. Sensor C registers a peak percentage variation of 152% between the third and the fourth minute, while sensor D records an even higher 232% after 4 min. The results suggest that CO_2 accumulates more quickly in the top section of the helmet (sensors A and B) than in the bottom (sensors C and D) during a flow-block. This may be due to sensors A and B being farther from the anti-suffocation valve, which reduces their exposure to the helmet's residual washout mechanism, leading to faster CO_2 buildup.

The SprintIR-6s sensor showed a significant increase in CO_2 concentration 5 min after a flow-block, as seen in Fig. 10. While this increase was less pronounced than with the SCD30 sensors, the SprintIR-6s, being close to the mannequin's mouth, is less affected by dilution, offering a more accurate measure of CO_2 levels in the localized area during the flow-block.

4.3. Limitations of the study and future directions

Despite the interesting and meaningful results, it must be recalled that the present study is far from being exhaustive and present several limitations. Firstly, it examined only a subset of potential CO_2 sensor positions within the NIV helmet. Exploring additional locations could provide a more comprehensive understanding of airflow dynamics inside the helmet, thus offering a better insight into the helmet behavior and providing guidelines for an optimal positioning of the sensor and for the improvement of the helmet geometry. In this concern, also the use of Computational Fluid Dynamics (CFD) simulations represents a promising path for enhancing our comprehension of airflow dynamics within the NIV helmet, contributing to the optimization of ventilation strategies.

Secondly, the study focused only on inlet tube blockage. Future research should explore additional scenarios, such as tube detachment or obstruction, to assess helmet performance under diverse conditions.

Thirdly, constant respiratory parameters were maintained during the evaluations. Exploring varying respiratory parameters and head movement effects in future analyses could provide a more detailed understanding of helmet performance across different clinical conditions. Incorporating these factors would lead to a more comprehensive assessment.

As we look to the future, there are several directions for further exploration and development in this field. Integrating CO_2 sensors can pave the way for the development of adaptive ventilation algorithms. These algorithms could automatically adjust ventilation settings in real-time based on detected CO_2 levels and patient needs, potentially optimizing treatment outcomes and patient comfort. Additionally, with the growing importance of telemedicine, incorporating CO_2 sensors into NIV helmets can be useful for remote patient monitoring. This application can extend the reach of critical care and improve access to respiratory treatment for patients in diverse settings. Finally, another potential future research direction is to leverage CFD simulations to improve our understanding of gas displacement within NIV helmets, with a particular focus on CO_2 distribution. This approach can help optimize ventilation strategies and inspire innovative designs for more effective and patient-centered solutions.

5. Conclusions

The study highlights the potential of integrating CO_2 sensors into NIV helmets to improve monitoring and enhance patient safety. The research provides valuable insights into the influence of fresh inlet gas flow rates and location of the sensor within the helmet, which can guide the design and optimization of NIV systems for better outcomes. Moreover, early detection of malfunctionings, such as flow blockages, by these sensors reduces the risk of CO_2 rebreathing and enhances patient safety.

This study revealed several key findings. Firstly, higher fresh inlet gas flow rates enhance CO_2 washout within the helmet, confirming prior research [4,15,21,22,31]. This emphasizes the importance of optimizing gas flow rates to minimize CO_2 rebreathing in NIV helmets. Secondly, the positioning of CO_2 sensors within the helmet significantly influences the measurement of local CO_2 concentration. The careful selection of an appropriate sensor location is pivotal in achieving a balance between signal stability and rapid response to flow-block events. Finally, the integration of a CO_2 sensor within the helmet holds significant potential as an alarm system designed to enhance patient safety and treatment effectiveness, capable of promptly alerting a flow-block event.

CRediT authorship contribution statement

Camilla Gironi: Writing – original draft, Methodology, Data curation, Conceptualization. **Ramin Amiri:** Writing – review & editing, Methodology, Data curation, Conceptualization. **Marco Giacinti Baschetti:** Writing – review & editing, Supervision, Methodology. **Cristiana Boi:** Writing – review & editing, Validation, Supervision. **Laura Cercenelli:** Writing – review & editing, Methodology. **Barbara Bortolani:** Writing – review & editing, Data curation. **Emanuela Marcelli:** Writing – review & editing, Validation, Supervision.

Table 3
P-values resulting from Student's t-test analysis for CO_2 concentration measurements acquired with SCD30 sensors A, B, C, D, E.

Time after flow block onset (min)	A	B	C	D	E
0.5	0.01	0.25	1.00	0.00	0.00
1	0.00	0.00	0.00	0.00	0.00
1.5	0.00	0.00	0.00	0.00	0.01
2	0.00	0.00	0.00	0.00	0.00
2.5	0.00	0.00	0.00	0.00	0.00
3	0.00	0.00	0.00	0.00	0.00
3.5	0.00	0.00	0.00	0.00	0.00
4	0.00	0.00	0.00	0.00	0.00
4.5	0.00	0.00	0.00	0.00	0.00
Time after flow block onset (min)	A	B	C	D	E
0.5	0.01	0.25	1.00	0.00	0.00
1	0.00	0.00	0.00	0.00	0.00
1.5	0.00	0.00	0.00	0.00	0.01
2	0.00	0.00	0.00	0.00	0.00
2.5	0.00	0.00	0.00	0.00	0.00
3	0.00	0.00	0.00	0.00	0.00
3.5	0.00	0.00	0.00	0.00	0.00
4	0.00	0.00	0.00	0.00	0.00
4.5	0.00	0.00	0.00	0.00	0.00

Data availability statement

The data that has been used is confidential.

Ethics statement

We have adhered to the Journal Ethics requirements, thus striving to contribute to a culture of integrity, fairness, and transparency in the scientific research community.

Duplicate and related publications

This submission represents original work and is not under consideration or review elsewhere. We confirm that there is no overlapping or redundant publication associated with this manuscript.

Preprints and inclusive language

We have ensured that our manuscript uses inclusive language that respects diversity and avoids discriminatory or exclusionary terms.

Image and data integrity

We have taken every measure to ensure the integrity of the images and data presented in this research. Images have not been manipulated in a way that could misrepresent findings. We confirm that no AI-generated or AI-altered images were used in this study.

Acknowledgement of sources

We have ensured that all relevant previous works have been cited appropriately to give due credit to colleagues and researchers whose work informed this study.

Use of AI in writing

AI technologies were not involved in decision-making, data analysis, or critical content creation for this research. AI tools have not been listed as authors, and any AI use has been transparently declared in the manuscript.

Declaration of competing interest

The authors declare that they have no known competing financial interests or personal relationships that could have appeared to influence the work reported in this paper.

Acknowledgments

The authors would like to thank Intersurgical S.p.a. for providing the NIV helmets used in this study and for the technical support.

References

[1] T. Piraino, Noninvasive respiratory support in acute hypoxemic respiratory failure, Respir. Care 64 (6) (giu. 2019) 638–646, https://doi.org/10.4187/respcare.06735.
[2] G. Cammarota, R. Simonte, e E. De Robertis, Comfort during non-invasive ventilation, Front. Med. 9 (2022) 874250, https://doi.org/10.3389/fmed.2022.874250.
[3] L. Vetrugno, C. Deana, N. Colaianni-Alfonso, F. Tritapepe, C. Fierro, e S.M. Maggiore, Noninvasive respiratory support in the perioperative setting: a narrative review, Front. Med. 11 (2024) 1364475, https://doi.org/10.3389/fmed.2024.1364475.
[4] G. Bello, P. De Santis, e M. Antonelli, Non-invasive ventilation in cardiogenic pulmonary edema, Ann. Transl. Med. 6 (18) (2018), https://doi.org/10.21037/atm.2018.04.39, 355–355, set.
[5] D. Chaudhuri, et al., Helmet noninvasive ventilation compared to facemask noninvasive ventilation and high-flow nasal cannula in acute respiratory failure: a systematic review and meta-analysis, Eur. Respir. J. 59 (3) (mar. 2022) 2101269, https://doi.org/10.1183/13993003.01269-2021.
[6] The Princeton Open Ventilation Monitor Collaboration, et al., Inexpensive multipatient respiratory monitoring system for helmet ventilation during COVID-19 pandemic, J. Med. Dev. Trans. ASME 16 (1) (mar. 2022) 011003, https://doi.org/10.1115/1.4053386.
[7] F. Menzella, et al., Effectiveness of noninvasive ventilation in COVID-19 related-acute respiratory distress syndrome, Clinical Respiratory J 15 (7) (lug. 2021) 779–787, https://doi.org/10.1111/crj.13361.
[8] L.S. Menga, C. Berardi, E. Ruggiero, D.L. Grieco, e M. Antonelli, Noninvasive respiratory support for acute respiratory failure due to COVID-19, Curr. Opin. Crit. Care 28 (1) (feb. 2022) 25–50, https://doi.org/10.1097/MCC.0000000000000902.
[9] J. Masip e A. Mas, «Noninvasive Ventilation in Acute Respiratory Failure», COPD, 2014, p. 837, https://doi.org/10.2147/COPD.S42664, ago.
[10] S. Alexiou, e H.B. Panitch, Physiology of non-invasive respiratory support, Semin. Fetal Neonatal Med. 21 (3) (giu. 2016) 174–180, https://doi.org/10.1016/j.siny.2016.02.007.
[11] S. Nava e N. Hill, «Non-invasive Ventilation in Acute Respiratory Failure», vol. 374, 2009.
[12] O. Chowdhury, C.J. Wedderburn, D. Duffy, e A. Greenough, CPAP review, Eur. J. Pediatr. 171 (fasc. 10) (2012) 1441–1448, https://doi.org/10.1007/s00431-011-1648-6.
[13] K.G. Buell e B.K. Patel, Helmet noninvasive ventilation in acute hypoxic respiratory failure, Curr. Opin. Crit. Care 29 (1) (feb. 2023) 8–13, https://doi.org/10.1097/MCC.0000000000001008.
[14] M. Cesarano, et al., Helmet noninvasive support for acute hypoxemic respiratory failure: rationale, mechanism of action and bedside application, Ann. Intensive Care 12 (fasc. 1) (2022) 94, https://doi.org/10.1186/s13613-022-01069-7, ott.
[15] N. Patroniti, G. Foti, A. Manfio, A. Coppo, G. Bellani, e A. Pesenti, Head helmet versus face mask for non-invasive continuous positive airway pressure: a physiological study, Intensive Care Med. 29 (10) (2003) 1680–1687, https://doi.org/10.1007/s00134-003-1931-8.
[16] T.A. Smith, P.M. Davidson, C.R. Jenkins, e J.M. Ingham, Life behind the mask: the patient experience of NIV, Lancet Respir. Med. 3 (1) (gen. 2015) 8–10, https://doi.org/10.1016/S2213-2600(14)70267-X.
[17] D. Chandra, et al., Outcomes of noninvasive ventilation for acute exacerbations of chronic obstructive pulmonary disease in the United States, 1998–2008, Am. J. Respir. Crit. Care Med. 185 (2) (gen. 2012) 152–159, https://doi.org/10.1164/rccm.201106-1094OC.
[18] J.-P. Frat, et al., High-flow oxygen through nasal cannula in acute hypoxemic respiratory failure, N. Engl. J. Med. 372 (23) (2015) 2185–2196, https://doi.org/10.1056/NEJMoa1503326.
[19] R. Vaschetto, et al., «A pragmatic, open-label, multi-center, randomized controlled clinical trial on the rotational use of interfaces vs standard of care in patients treated with noninvasive positive pressure ventilation for acute hypercapnic respiratory failure: the ROTAtional-USE of interface STUDY (ROTA-USE STUDY), Trials 24 (1) (ago. 2023) 527, https://doi.org/10.1186/s13063-023-07560-1.
[20] V. Squadrone et al., «Continuous Positive Airway Pressure for Treatment of Postoperative Hypoxemia».
[21] A. Coppadoro, E. Zago, F. Pavan, G. Foti, e G. Bellani, The use of head helmets to deliver noninvasive ventilatory support: a comprehensive review of technical aspects and clinical findings, Crit. Care 25 (1) (2021) 327, https://doi.org/10.1186/s13054-021-03746-8, dic.
[22] F. Mojoli, G.A. Iotti, M. Gerletti, C. Lucarini, e A. Braschi, Carbon dioxide rebreathing during non-invasive ventilation delivered by helmet: a bench study, Intensive Care Med. 34 (fasc. 8) (2008) 1454–1460, https://doi.org/10.1007/s00134-008-1109-5.
[23] P. Taccone, D. Hess, P. Caironi, e L.M. Bigatello, «Continuous positive airway pressure delivered with a “helmet”: effects on carbon dioxide rebreathing, Crit. Care Med. 32 (10) (2004) 2090–2096, https://doi.org/10.1097/01.CCM.0000142577.63316.C0.
[24] M.S. Siobal, Monitoring exhaled carbon dioxide, Respir. Care 61 (10) (ott. 2016) 1397–1416, https://doi.org/10.4187/respcare.04919.
[25] J.-M. Tonnelier, et al., Noninvasive continuous positive airway pressure ventilation using a new helmet interface: a case-control prospective pilot study, Intensive Care Med. 29 (11) (nov. 2003) 2077–2080, https://doi.org/10.1007/s00134-003-1925-6.
[26] N. Patroniti, M. Saini, A. Zanella, S. Isgrò, e A. Pesenti, Danger of helmet continuous positive airway pressure during failure of fresh gas source supply, Intensive Care Med. 33 (1) (gen. 2007) 153–157, https://doi.org/10.1007/s00134-006-0446-5.
[27] C. Chiappero, et al., Effectiveness and safety of a new helmet CPAP configuration allowing tidal volume monitoring in patients with COVID-19, Pulmonology 29 (dic. 2023) S9–S17, https://doi.org/10.1016/j.pulmoe.2021.06.012.
[28] A. Cortegiani, et al., Tidal volume estimation during helmet noninvasive ventilation: an experimental feasibility study, Sci. Rep. 9 (1) (nov. 2019) 17324, https://doi.org/10.1038/s41598-019-54020-5.
[29] E. Dervieux, M. Théron, e W. Uhring, Carbon dioxide sensing—biomedical applications to human subjects, Sensors 22 (1) (dic. 2021) 188, https://doi.org/10.3390/s22010188.
[30] T.K. Kim, T test as a parametric statistic, Korean J Anesthesiol 68 (6) (2015) 540, https://doi.org/10.4097/kjae.2015.68.6.540.
[31] F. Racca, et al., Helmet ventilation and carbon dioxide rebreathing: effects of adding a leak at the helmet ports, Intensive Care Med. 34 (8) (2008) 1461–1468, https://doi.org/10.1007/s00134-008-1120-x.